

The effect of strain rate on mechanical properties and fracture mode of the AZ31 alloy and commercially pure magnesium pre-exposed in a corrosive medium

© 2023

Evgeny D. Merson^{*1}, PhD (Physics and Mathematics),
senior researcher of the Research Institute of Advanced Technologies
*Vitaly A. Poluyanov*², PhD (Engineering),
junior researcher of the Research Institute of Advanced Technologies
*Pavel N. Myagkikh*³, junior researcher of the Research Institute of Advanced Technologies
*Dmitry L. Merson*⁴, Doctor of Sciences (Physics and Mathematics), Professor,
Director of the Research Institute of Advanced Technologies

Togliatti State University, Togliatti (Russia)

*E-mail: Mersoned@gmail.com

¹ORCID: <https://orcid.org/0000-0002-7063-088X>

²ORCID: <https://orcid.org/0000-0002-0570-2584>

³ORCID: <https://orcid.org/0000-0002-7530-9518>

⁴ORCID: <https://orcid.org/0000-0001-5006-4115>

Received 15.11.2022

Accepted 02.12.2022

Abstract: Magnesium alloys are promising materials for aviation, automotive engineering, and medicine, however, due to the low resistance to stress corrosion cracking (SCC), their wide application is limited. To create alloys with high resistance to SCC, a comprehensive study of this phenomenon nature is required. Previously, it was suggested that diffusible hydrogen and corrosion products formed on the magnesium surface can play an important role in the SCC mechanism. However, the contribution of each of these factors to the SCC-induced embrittlement of magnesium and its alloys is understudied. Since the influence of diffusible hydrogen on the mechanical properties of metals increases with the strain rate decrease, the study of the strain rate sensitivity of the SCC-susceptibility of magnesium alloys is a critical task. In this work, the authors studied the effect of the strain rate in the range from $5 \cdot 10^{-6}$ to $5 \cdot 10^{-4} \text{ s}^{-1}$ on the mechanical properties, the state of the side and fracture surfaces of the as-cast commercially pure magnesium and the AZ31 alloy before and after exposure to a corrosive environment and after removal of corrosion products. The study identified that the preliminary exposure to a corrosive medium leads to the AZ31 alloy embrittlement, but does not affect the mechanical properties and the fracture mode of pure magnesium. The authors found that the AZ31 alloy embrittlement caused by the preliminary exposure to a corrosive medium appears extensively only at the low strain rate and only if the layer of corrosion products is present on the specimens' surface. The study shows that a change in the strain rate has little effect on the mechanical properties of pure magnesium. The authors concluded that the main cause of the AZ31 alloy embrittlement after soaking in a corrosive medium is the corrosion products layer, which presumably contains the embrittling agents such as hydrogen and residual corrosive medium.

Keywords: magnesium alloys; AZ31; pure magnesium; stress corrosion cracking; corrosion; strain rate; mechanical properties.

Acknowledgements: The research is financially supported by the Russian Science Foundation within the scientific project No. 18-19-00592.

For citation: Merson E.D., Poluyanov V.A., Myagkikh P.N., Merson D.L. The effect of strain rate on mechanical properties and fracture mode of the AZ31 alloy and commercially pure magnesium pre-exposed in a corrosive medium. *Frontier Materials & Technologies*, 2023, no. 3, pp. 71–82. DOI: 10.18323/2782-4039-2023-3-65-7.

INTRODUCTION

The impact of a corrosive environment on a metal, to which an external or internal mechanical stress is applied, facilitates the initiation and propagation of cracks. This phenomenon referred to as stress corrosion cracking (SCC) is a common cause of a sudden failure of elements of industrial equipment and structures, as well as other metal goods operating in contact with an aggressive environment. At best, the failure of one or another part causes economic losses, for example, associated with the stoppage of production and repair process, and at worst, it leads to techno-catastrophes often accompanied by human losses. Most structural metals and alloys are susceptible to this harmful phenomenon, including carbon and stainless steels, alloys based on copper, titanium, aluminum, magnesium, and many others.

Recently, special emphasis has been paid to the issue of SCC of magnesium alloys. Since these materials have the highest specific strength among known structural alloys, they are of great interest for the aircraft and automotive industries, as well as for other industries where the product weight is one of the most important parameters. However, the operating conditions of a large number of vehicles, including ground and air transport vehicles, are favorable for the SCC development since these conditions involve the contact of loaded parts with aggressive media, for example, salt water or humid air.

Moreover, the application of magnesium alloys in medical bioresorbable implants that can dissolve in the human body without harming it is actively developing. The use of these products, for example, in the form of plates and screws for fixing bone fragments in fractures, allows avoiding

a repeated operation, which is usually required after the end of treatment to remove traditional insoluble temporary implants made of titanium or stainless steels. Being in the natural internal environment of the human body that is aggressive towards magnesium, an implant constantly experiences static and alternating loads. Since the cross section gradually decreases as the device dissolves, such operating conditions are associated with a particularly high risk of premature brittle fracture of the implant due to SCC.

Thus, the production of magnesium alloys with an increased SCC resistance is a critical task, the solution of which requires a comprehensive study of this phenomenon nature. In the issue of choosing the approaches to the formation of a microstructure with the high SCC resistance, understanding the mechanisms of the crack initiation and propagation in a corrosive environment is of key importance. Many works show that the nucleation of cracks during SCC occurs on elongated corrosion pits, which are formed by the magnesium local anodic dissolution [1; 2]. However, currently, the mechanism of further crack propagation is not unanimous. Most researchers tend to believe that the growth of cracks in magnesium alloys under the SCC conditions is controlled by the diffusible hydrogen, which penetrates into the metal as a result of the cathodic reaction of hydrogen reduction occurring on the magnesium surface in aqueous corrosion solutions [3; 4]. The following arguments are given in favor of this hypothesis. Firstly, using gas analysis, it was experimentally shown that soaking in a corrosive medium leads to an increase in the hydrogen concentration in pure magnesium [5], as well as in the Mg-7.5%Al [6], AZ31, and ZK60 alloys [5; 7]. Secondly, it has been identified that pure magnesium [8], as well as some of magnesium alloys, including AZ31 [7], AZ91 [9], AZ80 [10], ZK21 [11], ZK60 [7], Mg-2Zn-1Nd-0.6Zr [12], and others [13-15] suffer embrittlement, called pre-exposure SCC (PESCC), which manifests itself upon tension in air, if before testing, specimens of these materials were kept in a corrosive environment. Thirdly, the degree of embrittlement as a result of PESCC decreases with increasing strain rate [16], which is one of the characteristic features of hydrogen embrittlement of many metals and alloys, for example, steels and aluminum alloys [17; 18]. Fourthly, as is the case with hydrogen embrittlement, PESCC of magnesium alloys can be partially or completely eliminated by keeping samples in air or in vacuum at room or elevated temperature after exposure to a corrosive environment [19; 20].

At first sight, the specified features of SCC and PESCC of magnesium alloys are actually very similar to the features of hydrogen embrittlement observed in other metals, which invited the researchers' assumption about the analogy of the mechanisms controlling these phenomena. Nevertheless, the results of a number of recent studies have shown that SCC and PESCC of magnesium alloys can also develop in the absence of diffusible hydrogen in their bulk. So, the works [5; 7] identified that the diffusible hydrogen concentration in the samples of pure magnesium, as well as of the AZ31 and ZK60 alloys, which were subject to the PESCC tests or exposure to a corrosive environment, was negligible if the corrosion products were removed from the surface of samples before gas analysis (which was not done in earlier works). Moreover, it was found that the removal of a layer of corrosion products from the samples of

the AZ31 and ZK60 alloys exposed to a corrosive environment leads to the complete restoration of their mechanical properties and the elimination of any PESCC signs, including a strain rate dependence of the loss of ductility in the ZK60 alloy [7; 16]. Thus, it was proved that a corrosion products' layer formed on the alloy surface when interacting with a corrosive medium can play a key role in the PESCC mechanism. In [16], it was assumed that this layer acts as a container for "embrittling agents", in particular, hydrogen and residual corrosion medium, which, during the crack growth, can diffuse through the crack volume to its tip contributing to its propagation. The presence of a corrosive medium, as well as hydrogen, in the corrosion products' layer in the ZK60 alloy was experimentally confirmed in the work [20].

At the same time, the suppression of the PESCC of magnesium alloys with an increase in the strain rate probably indicates that the crack growth rate is limited by the rate of diffusion of embrittling agents from the surface to the tip of this crack. However, studies of the strain rate effect on the PESCC of magnesium alloys, especially after the removal of corrosion products, have hardly been carried out. In fact, data of this kind are presented in the literature only for the ZK60 alloy [16]. Therefore, to increase the reliability of the results of previous works and the conclusions about the SCC and PESCC mechanisms based on these results, it is necessary to carry out similar tests for other magnesium alloys, as well as for pure magnesium.

The work was aimed to clarify the PESCC nature of magnesium alloys by studying the effect of the strain rate and corrosion products on the mechanical properties and fracture surface of the AZ31 alloy and technically pure magnesium.

METHODS

The research was carried out using the samples of the as-cast technically pure magnesium and the AZ31 commercial alloy samples in the form of a hot-rolled sheet. The chemical composition of the selected materials shown in Table 1 was identified using the ARL 4460 optical-emission spectrometer (Thermo Fisher Scientific). An average size of a pure magnesium grain and the AZ31 alloy α -phase was 3 mm and 10 μm respectively. The microstructure of the selected materials was considered in previous works [5].

Threaded cylindrical specimens for tensile tests with a working part of 30×6 mm in size were produced by turning blanks. The specimens were cut along the rolling direction (AZ31) or along the cast slab axis (pure magnesium). The working part of prepared specimens was soaked in an aqueous corrosion solution of 4 % NaCl + 4 % $\text{K}_2\text{Cr}_2\text{O}_7$ for 24 hours. The soaking in the corrosion media was carried out at room temperature (24 °C) without applying the external mechanical and electrical stress. After that, the specimens were removed out of the corrosion solution, washed in an ethylic alcohol jet, and then dried with compressed air.

Mechanical tests of specimens pre-exposed to a corrosive environment were carried out in air at room temperature according to the uniaxial tension scheme at constant initial strain rate of $5 \cdot 10^{-6}$ and $5 \cdot 10^{-4} \text{ s}^{-1}$ (0.01 and 1 mm/min) using the AG-Xplus testing machine (Shimadzu).

Table 1. Chemical composition of the AZ31 alloy and technically pure magnesium, % wt.
Таблица 1. Химический состав сплава AZ31 и технически чистого магния, вес. %

Material	Mg	Al	Zn	Ca	Zr	Fe	Cu	Mn	Ce	Nd	Si
AZ31	Base	4.473	0.887	0.0015	–	0.002	0.003	0.312	0.017	0.007	0.008
Pure magnesium	Base	0.005	–	0.0002	–	0.067	–	0.002	0.009	0.001	0.003

To compare, similar tests were conducted for specimens in the reference state, previously not subjected to exposure to a corrosive environment, and for specimens pre-exposed to a corrosive environment, from the surface of which corrosion products were removed immediately after exposure. The removal of corrosion products was performed by dipping a specimen for 1 minute to the standard C.5.4 (20 % CrO₃ + 1 % AgNO₃) solution according to the GOST R 9.907-2007 standard. After removing the corrosion products, the specimens were washed in alcohol and dried with compressed air. After mechanical tests, the fractures and side surfaces of fractured specimens were analyzed using the JCM-6000 scanning electron microscope (JEOL).

RESULTS

Mechanical properties

As a result of the experiments, it was found that an increase in the strain rate of samples of the AZ31 alloy in the reference state leads to a decrease in their ductility and an increase in strength (Fig. 1 a, 1 b, 2 a). The tests at a low strain rate showed that preliminary holding of samples of this alloy in a corrosive environment leads to a decrease both in its strength and ductility (Fig. 1 a, 1 b, 2 a). However, at a high strain rate, there is no decrease in mechanical properties after corrosion exposure. Moreover, the complete restoration of the alloy mechanical properties occurs if, after soaking in a corrosive environment, corrosion products are removed from the surface of the samples. This effect is observed both at low and high strain rates.

The ductility of the reference pure magnesium samples slightly depends on the strain rate, and the increase in the strength with increasing strain rate is much weaker than that of the AZ31 alloy (Fig. 1 c, 1 d, 2 b). Preliminary exposure to a corrosive environment does not have a significant effect on the pure magnesium ductility, but leads to a slight decrease in its strength, which slightly increases with an increase in the strain rate. Interestingly, the ductility of pure magnesium specimens with the removed corrosion products is significantly lower than that of specimens in the reference state and specimens kept in a corrosive environment, from the surface of which corrosion products were not removed.

The analysis of fractures and side surfaces

On the side surface of the AZ31 alloy specimens (Fig. 3) tested for tension in the initial state, a large number of small ductile cracks oriented across the tension axis are

observed (Fig. 3 a, 3 d). These cracks appear along the grooves formed by the cutter on the metal surface during turning. On the surface of the samples that were subjected to soaking in a corrosive environment followed by a tensile test at a low strain rate, there are also many cracks, which, however, are much larger and more brittle compared to cracks on the reference samples (Fig. 3 b). After testing at a high strain rate, there are practically no such large cracks in specimens of a similar type (Fig. 3 e). Large cracks are present on the surface of samples from which the corrosion products were removed before testing, but their quantity is significantly less than that of samples that were tested after holding in the environment without removing the corrosion products (Fig. 3 c).

The fractographic analysis (Fig. 4) showed that the fractures of the AZ31 alloy reference samples are fully-ductile, regardless of the strain rate (Fig. 4 a, 4 d). On the fracture surface of specimens tested at a low strain rate and after pre-exposure to a corrosive medium, together with the dominant ductile component, there are multiple brittle fracture areas, which are always located in the peripheral part of the fracture and directly adjacent to the side surface of the specimen (Fig. 4 b). One of these brittle areas is blocked with a frame ("A" area in Fig. 4 b) and is shown at higher magnification in Fig. 5 a.

On the fracture surface of specimens with the removed corrosion products tested at a low strain rate, there are also a small amount of such brittle fracture areas (Fig. 4 c and 5 b); however, their quantity is significantly less than in specimens from which the corrosion products were not removed. The fractures of all specimens pre-exposed to a corrosive environment and tested at a high strain rate are fully-ductile and do not contain brittle fracture areas, regardless of whether the corrosion products were removed from them or not (Fig. 4 d–f).

On the side surface of pure magnesium specimens tested in the reference state and after soaking in a corrosive environment, including the subsequent removal of corrosion products, there are large cracks and numerous slip bands (Fig. 6). Moreover, a network of small cracks is also observed on the surface of specimens pre-exposed to a corrosive environment (Fig. 6 e and 7 a). Interestingly, there is a large quantity of corrosion pits on the surface of samples with the removed corrosion products (Fig. 6 c, 6 f, and 7 b), which are not observed on the surface of samples tested immediately after soaking in a corrosive environment (without the removal of corrosion products). No critical effect of the strain rate on the appearance of the side surface of pure magnesium specimens in the initial state and after soaking in a corrosive medium was found.

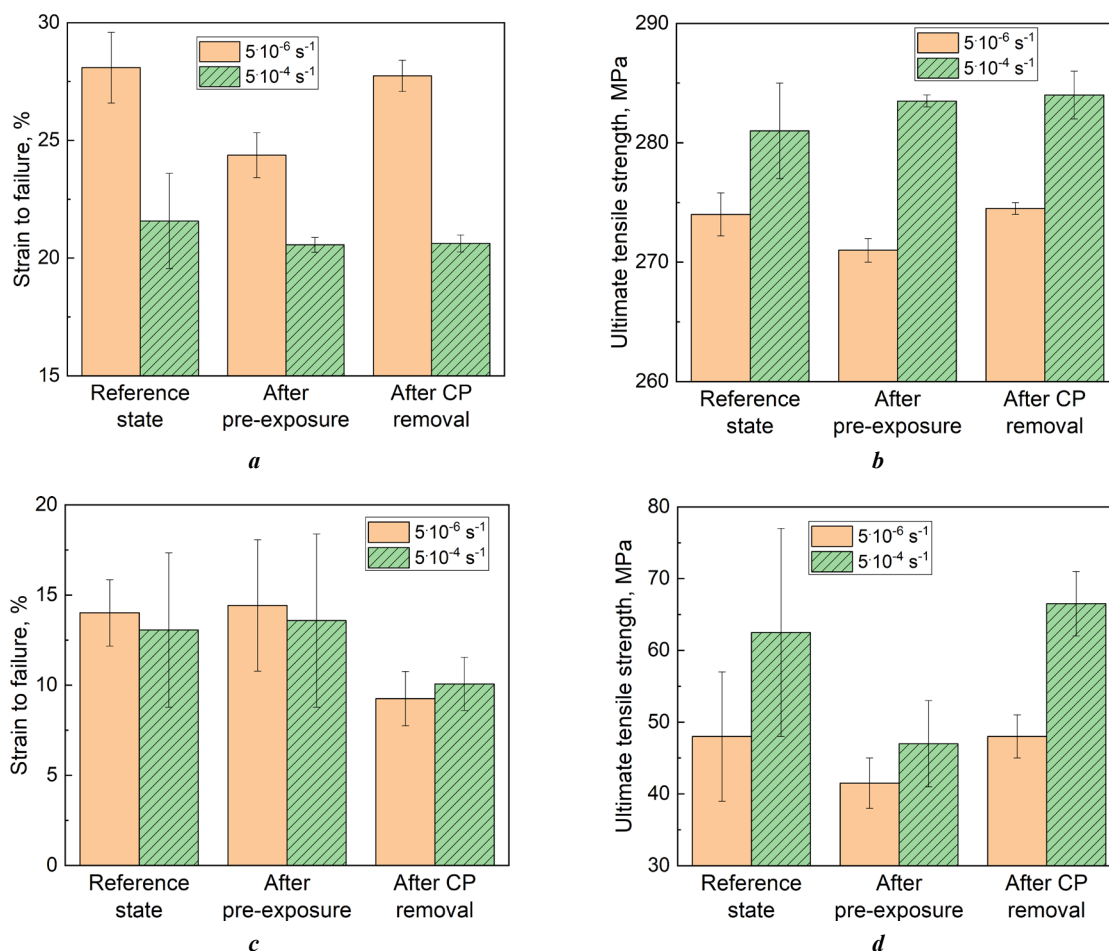


Fig. 1. The effect of strain rate on elongation to failure (a, c) and ultimate tensile strength (b, d) of the AZ31 alloy specimens (a, b) and technically pure magnesium specimens (c, d) in the reference state, after the pre-exposure to a corrosive medium, and after the pre-exposure to a corrosive medium followed by the removal of corrosion products

Рис. 1. Влияние скорости деформирования на деформацию до разрушения (a, c) и предел прочности (b, d) образцов сплава AZ31 (a, b) и технически чистого магния (c, d) в исходном состоянии, после выдержки в коррозионной среде и после выдержки в коррозионной среде с последующим удалением продуктов коррозии

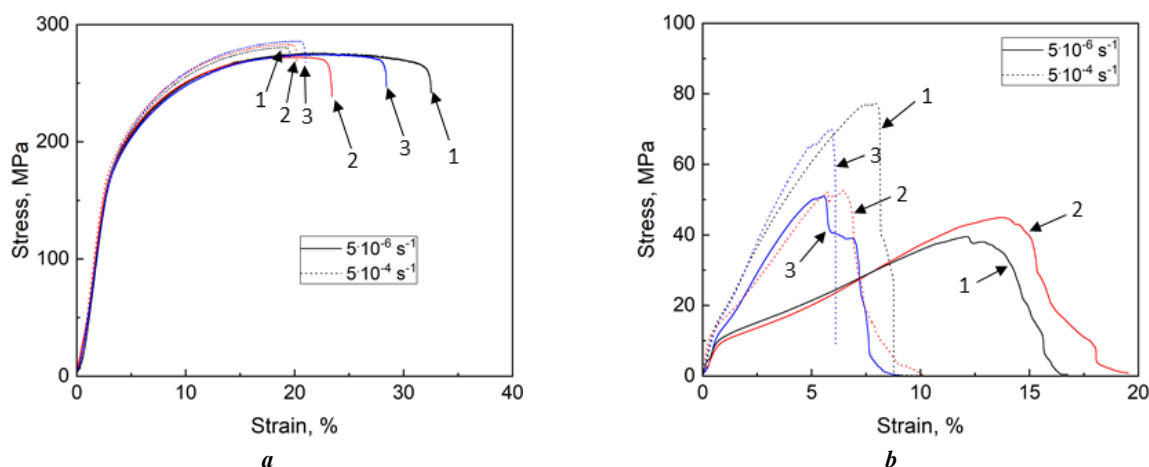


Fig. 2. The effect of strain rate on the stress-strain diagrams of the AZ31 alloy specimens (a) and technically pure magnesium specimens (b) in different states: 1 – reference state; 2 – after the pre-exposure to a corrosive medium; 3 – after the pre-exposure to a corrosive medium and the removal of corrosion products

Рис. 2. Влияние скорости деформирования на диаграммы растяжения образцов сплава AZ31 (a) и технически чистого магния (b) в разных состояниях: 1 – исходном; 2 – после предварительной выдержки в коррозионной среде; 3 – после предварительной выдержки в коррозионной среде и удаления продуктов коррозии

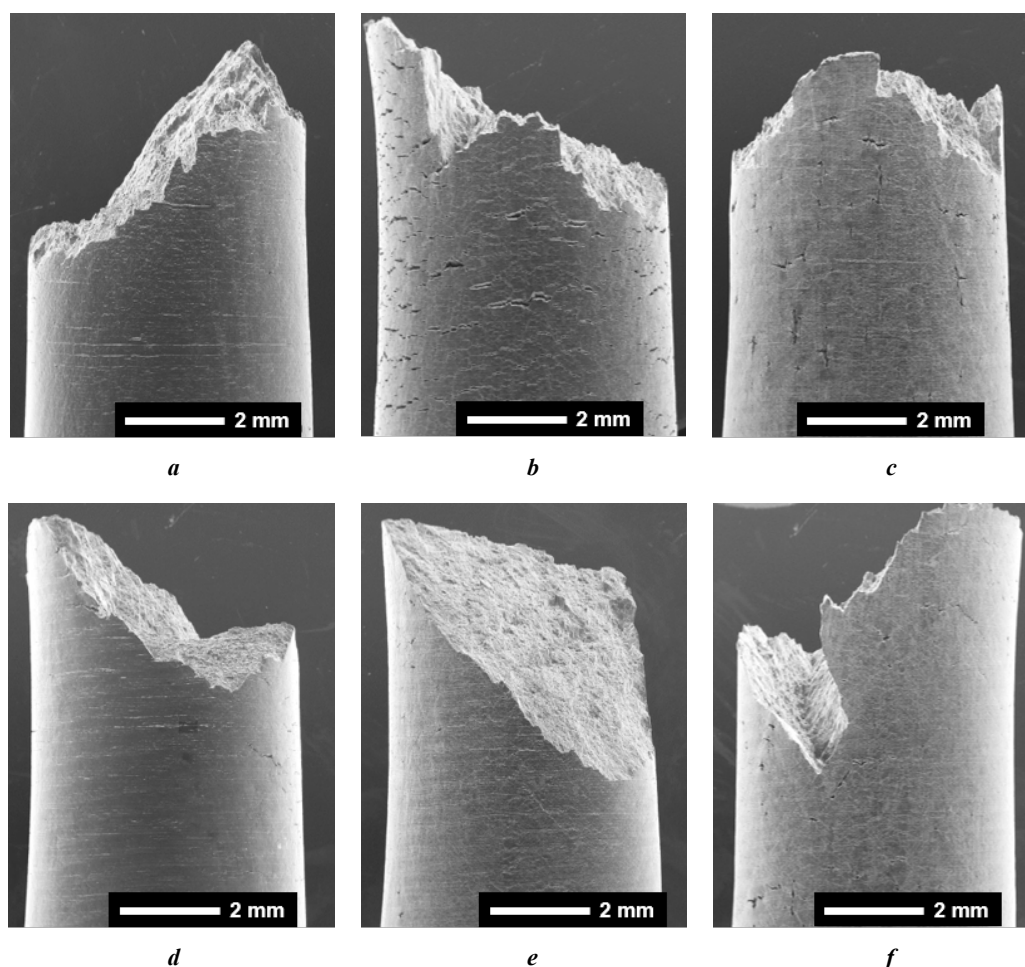


Fig. 3. The appearance of the side surface of the AZ31 alloy specimens tensile-tested in air: **a, d** – in the reference state; **b, e** – after the pre-exposure to a corrosive medium; **c, f** – after the pre-exposure to a corrosive medium and the removal of corrosion products: **a–c** – at a low ($5 \cdot 10^{-6} \text{ s}^{-1}$) strain rate; **d–f** – at a high ($5 \cdot 10^{-4} \text{ s}^{-1}$) strain rate. Images are obtained by SEM

Рис. 3. Внешний вид боковой поверхности образцов сплава AZ31, испытанных на растяжение на воздухе: **a, d** – в исходном состоянии; **b, e** – после выдержки в коррозионной среде; **c, f** – после выдержки в коррозионной среде и удаления продуктов коррозии при: **a–c** – низкой ($5 \cdot 10^{-6} \text{ с}^{-1}$); **d–f** – высокой ($5 \cdot 10^{-4} \text{ с}^{-1}$) скоростях деформирования. Снимки получены при помощи СЭМ

The fracture surface of all pure magnesium samples has a similar structure, regardless of the strain rate and the type of samples (Fig. 8). In all cases, the fracture is represented mainly by the facets with a fluted relief. Smooth facets without clearly defined relief are occasionally found.

DISCUSSION

The results obtained in the work showed that the loss of the AZ31 alloy mechanical properties as a result of PESCC can be completely eliminated when increasing the strain rate by two orders of magnitude, from $5 \cdot 10^{-6}$ to $5 \cdot 10^{-4} \text{ s}^{-1}$. A similar result was previously obtained for the ZK60 alloy [16] when exposing it to a medium of the same composition and at the same strain rates as in the present work. Usually, such behavior of mechanical characteristics depending on the strain rate is explained by the embrittling effect of diffusible hydrogen, which weakens with an increase in the strain rate.

A negative strain rate dependence of the ductility loss was identified in many metallic hydrogen-saturated materials, for example, in steels [18] and aluminum-based alloys

[17]. In these works, such behavior of ductility depending on the strain rate can only be explained by the effect of hydrogen dissolved in the bulk of the metal, since hydrogenation was carried out without corrosion participation. However, when discussing the nature of the negative strain rate dependence of the loss of ductility of magnesium alloys embrittled as a result of interaction with a corrosive medium, it is necessary, along with the possible hydrogen dissolution in the bulk of the metal, to consider other factors, for example, the presence of corrosion products on the surface of samples, which may contain both hydrogen and residual corrosive medium in liquid form.

Indeed, the results of the present study for the AZ31 alloy, as well as of the previous studies for the ZK60 alloy, show that the removal of a layer of corrosion products from the surface of samples before tensile testing eliminates both the embrittlement caused by preliminary exposure to a corrosive environment and the negative strain rate sensitivity of ductility loss associated with this embrittlement. In this case, the loss of ductility of samples with the removed corrosion products either increases with an increase in the strain rate (ZK60 alloy) or does not depend on the latter (AZ31 alloy).

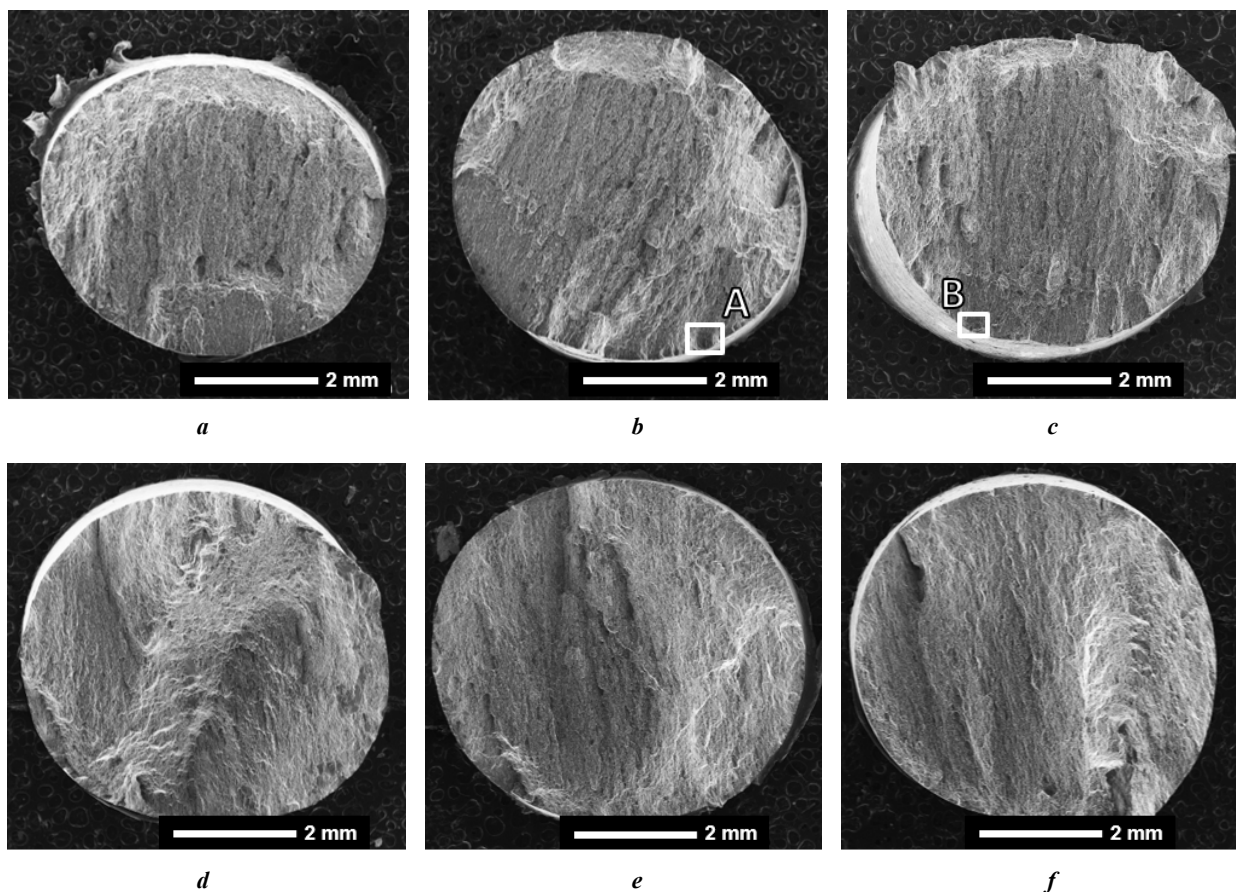


Fig. 4. The appearance of the fracture surface of the AZ31 alloy specimens tensile- tested in air: **a, d** – in the reference state; **b, e** – after the pre-exposure to a corrosive medium; **c, f** – after the pre-exposure to a corrosive medium and the removal of corrosion products: **a–c** – at a low ($5 \cdot 10^{-6} \text{ s}^{-1}$) strain rate; **d–f** – at a high ($5 \cdot 10^{-4} \text{ s}^{-1}$) strain rate.

Images are obtained by SEM. The blocked "A" and "B" areas are shown in Figure 5

Рис. 4. Внешний вид изломов образцов сплава AZ31, испытанных на растяжение на воздухе: **a, d** – в исходном состоянии; **b, e** – после выдержки в коррозионной среде; **c, f** – после выдержки в коррозионной среде и удаления продуктов коррозии при: **a–c** – низкой ($5 \cdot 10^{-6} \text{ с}^{-1}$); **d–f** – высокой ($5 \cdot 10^{-4} \text{ с}^{-1}$) скоростях деформирования.

Снимки получены при помощи СЭМ. Выделенные области «А», «В» представлены на рис. 5

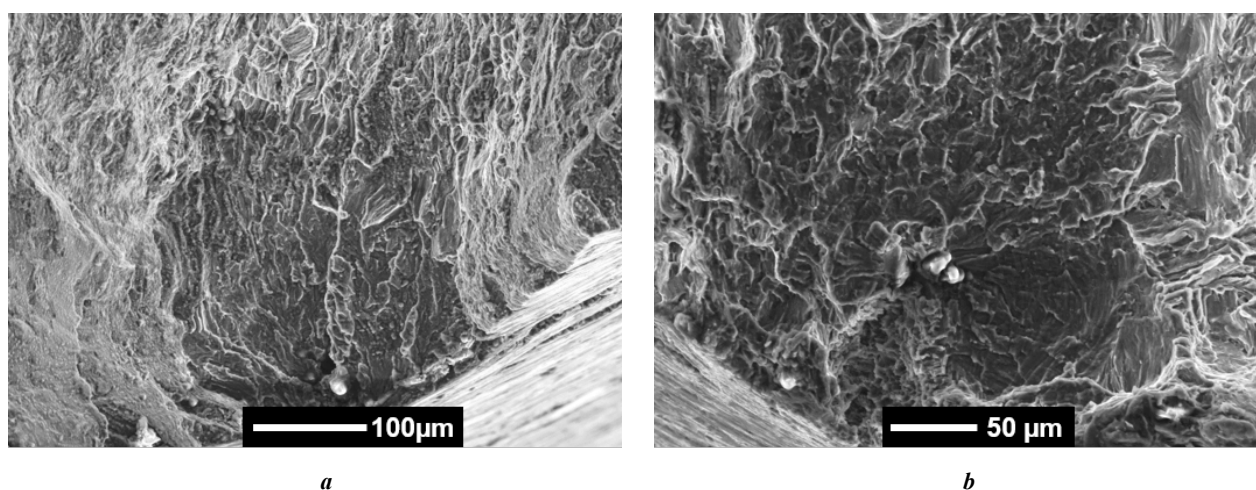


Fig. 5. The magnified fracture surface areas blocked in the frames in fig. 4 b and 4 c, respectively: **a** – "A" area; **b** – "B" area, containing the regions of brittle fracture in the peripheral part of the fracture surfaces of the AZ31 alloy specimens tested at a low strain rate immediately after the pre-exposure to a corrosive medium (**a**) and after the removal of corrosion products (**b**). Images are obtained by SEM

Рис. 5. Увеличенные области поверхности разрушения, обведенные рамками на рис. 4 b и 4 c соответственно:

a – область «А»; **b** – область «В», содержащие участки хрупкого разрушения в периферийной части излома образцов сплава AZ31. Образцы испытывались при низкой скорости деформирования сразу после выдержки в коррозионной среде (**a**) и после удаления продуктов коррозии (**b**). Снимки получены при помощи СЭМ

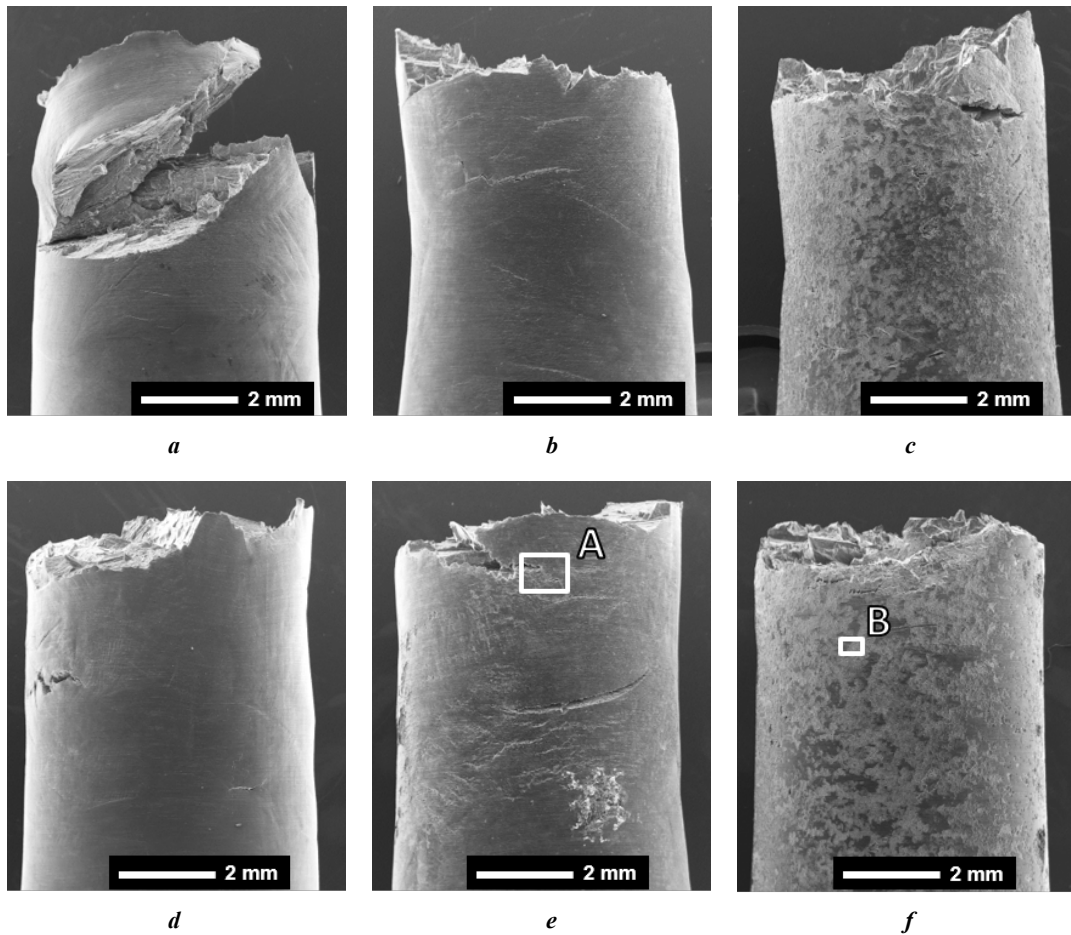


Fig. 6. The appearance of the side surface of the technically pure magnesium specimens tensile-tested in air: **a, d** – in the reference state; **b, e** – after the pre-exposure to a corrosive medium; **c, f** – after the pre-exposure to a corrosive medium and the removal of corrosion products: **a–c** – at a low ($5 \cdot 10^{-6} \text{ s}^{-1}$) strain rate; **d–f** – at a high ($5 \cdot 10^{-4} \text{ s}^{-1}$) strain rate.

Images are obtained by SEM. The blocked "A" and "B" areas are shown in Figure 7

Рис. 6. Внешний вид боковой поверхности образцов технического чистого магния, испытанных на растяжение на воздухе: **a, d** – в исходном состоянии; **b, e** – после выдержки в коррозионной среде; **c, f** – после выдержки в коррозионной среде и удаления продуктов коррозии при: **a–c** – низкой ($5 \cdot 10^{-6} \text{ с}^{-1}$); **d–f** – высокой ($5 \cdot 10^{-4} \text{ с}^{-1}$) скоростях деформирования. Снимки получены при помощи СЭМ. Выделенные области «А», «В» представлены на рис. 7

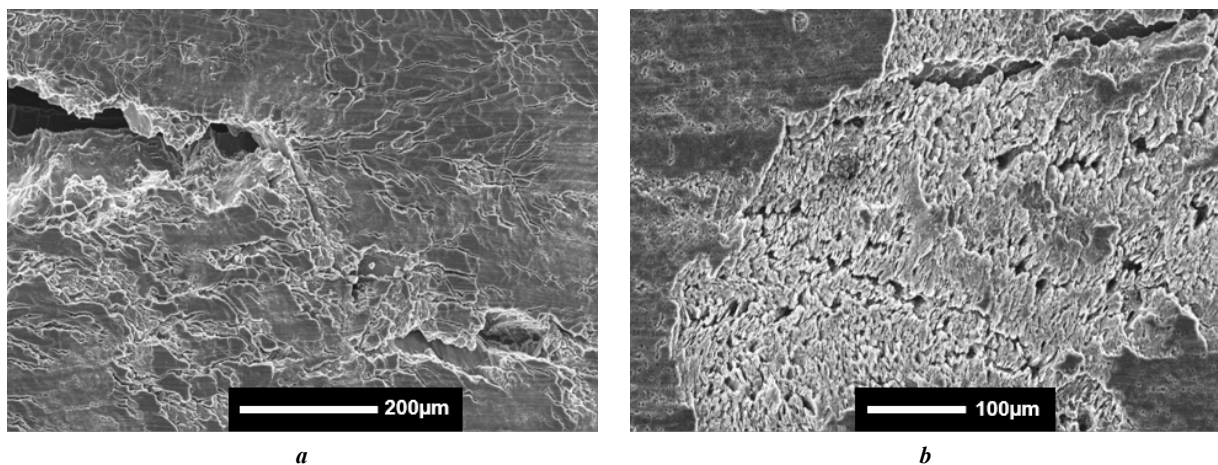


Fig. 7. The magnified side surface areas blocked in the frames in fig. 6 e and 6 f respectively: **a** – "A" area; **b** – "B" area, illustrating the brittle cracks net (**a**) and corrosion pits (**b**) on the surface of technically pure magnesium specimens tested at the low strain rate right after pre-exposure to corrosive medium – **a**; as well as after the removal of corrosion products – **b**. The images are obtained by SEM

Рис. 7. Увеличенные области боковой поверхности, обведенные рамками на рис. 6 e и 6 f соответственно: **a** – область «А»; **b** – область «В», иллюстрирующие сетку хрупких трещин (**a**) и коррозионные язвы (**b**) на поверхности образцов технического чистого магния. Образцы испытывались при высокой скорости деформирования сразу после выдержки в коррозионной среде (**a**) и после удаления продуктов коррозии (**b**). Снимки получены при помощи СЭМ

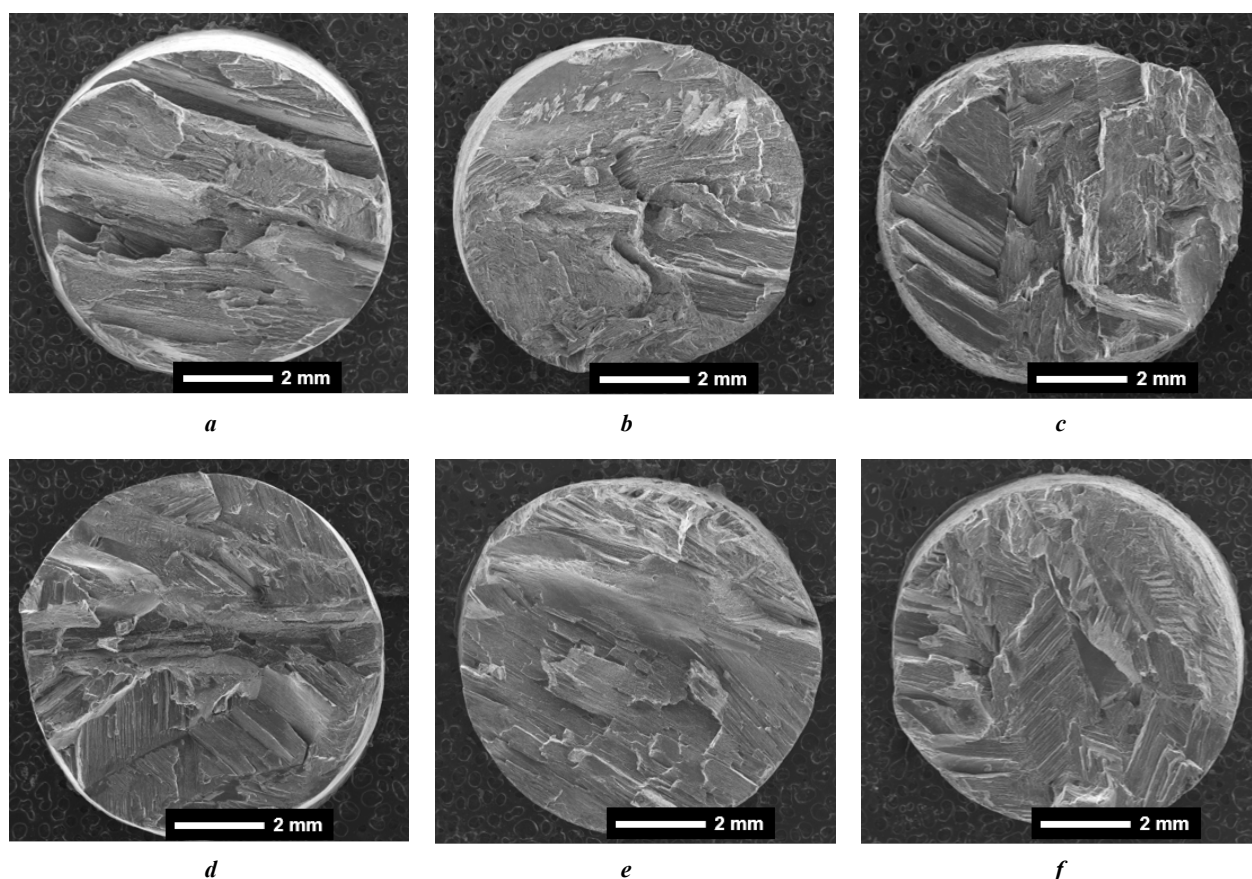


Fig. 8. The appearance of the fracture surface of the technically pure magnesium specimens tensile-tested in air: *a, d* – in the reference state; *b, e* – after the pre-exposure to a corrosive medium; *c, f* – after the pre-exposure to a corrosive medium and the removal of corrosion products: *a–c* – at a low ($5 \cdot 10^{-6} \text{ s}^{-1}$) strain rate; *d–f* – at a high ($5 \cdot 10^{-4} \text{ s}^{-1}$) strain rate.

Images are obtained by SEM

Рис. 8. Внешний излом образцов технического чистого магния, испытанных на растяжение на воздухе: *a, d* – в исходном состоянии; *b, e* – после выдержки в коррозионной среде; *c, f* – после выдержки в коррозионной среде и удаления продуктов коррозии при: *a–c* – низкой ($5 \cdot 10^{-6} \text{ с}^{-1}$); *d–f* – высокой ($5 \cdot 10^{-4} \text{ с}^{-1}$) скоростях деформирования. Снимки получены при помощи СЭМ

The suppression of the AZ31 alloy embrittlement as a result of the removal of corrosion products is confirmed, firstly, by the restoration of mechanical properties at a low strain rate, and secondly, by a significant decrease in the number of large brittle cracks on the side surface of samples, as well as the areas with the brittle fracture morphology on the fracture surfaces of these samples. In fairness, it should be noted that a small quantity of cracks and brittle fracture areas in the AZ31 alloy samples is still present even after the removal of corrosion products. Hypothetically, this may be associated with the incomplete removal of corrosion products. The work [7] showed that C.5.4 solution used in the present and previous works is noticeably less effective in removing corrosion products from the AZ31 alloy than from the ZK60 alloy. It can be assumed that hydrogen still partially penetrates into the metal surface layer. However, it is not clear why this does not occur in the ZK60 alloy, which, all other things being equal, as a result of soaking in a corrosive environment, is embrittled much more strongly than the AZ31 alloy, but does not show any signs of embrittlement after the removal of corrosion products [7]. It can be concluded that the key role in the PESCC mechanism of the AZ31

alloy is played by the layer of corrosion products, which presumably contains the “embrittling agents” such as hydrogen and residual corrosive environment. Probably, the participation of these agents in the mechanism of crack initiation and growth, including their diffusion from the sample surface to the crack tip, leads to the appearance of a negative rate sensitivity of ductility. At the same time, as shown by previous studies, the hydrogen penetration directly into the bulk of the magnesium matrix almost does not occur during the corrosion process [5; 7].

In view of the above reasoning, it is interesting that technically pure magnesium is actually not subject to the PESCC process – at least in the as-cast coarse-grained state and when exposed to a corrosive solution of the 4 % NaCl + 4 % K₂Cr₂O₇ composition. At the same time, in the literature, there is evidence that fine-grained magnesium suffers embrittlement after soaking in the 10⁻³ M Na₂SO₄ solution [8]. Coarse-grained magnesium is also distinguished by the almost complete absence of ductility strain rate sensitivity both in the reference state and after pre-exposure to a corrosive environment.

In spite of the fact that the actual reason for the high resistance of this material to PESCC has yet to be investigat-

ed, at the moment two possible explanations for this phenomenon can be proposed. Firstly, the presence of secondary phases in the structure can be a critical factor affecting the stability of a particular magnesium alloy. It is known that particles of almost all secondary phases in magnesium alloys act as a cathode in relation to the magnesium matrix and, therefore, serve as the sites for the initiation of corrosion pits [21], which subsequently act as the crack nuclei during SCC [1]. Consequently, the absence of such particles in pure magnesium can favorably affect its resistance to PESCC and SCC. Secondly, one can assume that the pure magnesium immunity to PESCC is associated with its low strength. The pure magnesium plastic deformation begins at very low stresses, so even if brittle cracks have time to nucleate, they quickly become blunted due to the plastic flow at their tips and propagate mainly by a ductile mechanism. Indeed, numerous small brittle cracks were found on the lateral surface of magnesium specimens kept in a corrosive medium. However, the fractures of these samples, as well as of samples in the reference state, are mainly represented by facets with a characteristic fluted pattern, which is formed due to the formation and ductile merging of tubular pores [22], which indicates a ductile mechanism of crack propagation in this material.

It is important to note that pure magnesium samples, from which the corrosion products were removed after soaking in a corrosive medium, have noticeably lower ductility than samples, from which corrosion products were not removed. Probably, it is associated with the presence of corrosion pits, which were identified on the side surface of the samples after the removal of corrosion products. Apparently, the standard C.5.4 solution for removing corrosion products can lead to corrosion damage to pure magnesium, although this was not observed when interacting with the AZ31 and ZK60 alloys. Currently, it is unclear whether this effect depends on the presence and type of corrosion products on the surface of pure magnesium.

CONCLUSIONS

1. An increase in the strain rate from $5 \cdot 10^{-6}$ to $5 \cdot 10^{-4} \text{ s}^{-1}$ leads to a complete elimination of the AZ31 alloy embrittlement caused by preliminary exposure to an aqueous solution of the 4 % NaCl + 4 % $\text{K}_2\text{Cr}_2\text{O}_7$ composition for 24 h.

2. The removal of corrosion products using the standard C.5.4 (20 % CrO_3 + 1 % AgNO_3) solution from the surface of the AZ31 alloy pre-exposed to a corrosive environment leads to a complete elimination of the loss of ductility caused by PESCC, but does not completely suppress brittle cracking.

3. Technically pure magnesium in the as-cast coarse-grained condition is not susceptible to PESCC after soaking in an aqueous solution of the 4 % NaCl + 4 % $\text{K}_2\text{Cr}_2\text{O}_7$ composition for 24 h.

4. An increase in the strain rate from $5 \cdot 10^{-6}$ to $5 \cdot 10^{-4} \text{ s}^{-1}$ has no significant effect on the mechanical properties of technically pure magnesium in the as-cast coarse-grained state, regardless of whether preliminary exposure to a corrosive medium was carried out before the tensile tests or not.

REFERENCES

1. Yu Z., Chen J., Yan H., Xia W., Su B., Gong X., Guo H. Degradation, stress corrosion cracking behavior and cytocompatibility of high strain rate rolled Mg-Zn-Sr alloys. *Materials Letters*, 2020, vol. 260, article number 126920. DOI: [10.1016/j.matlet.2019.126920](https://doi.org/10.1016/j.matlet.2019.126920).
2. Zhang X., Wu W., Fu H., Li J. The effect of corrosion evolution on the stress corrosion cracking behavior of mooring chain steel. *Corrosion Science*, 2022, vol. 203, article number 110316. DOI: [10.1016/j.corsci.2022.110316](https://doi.org/10.1016/j.corsci.2022.110316).
3. Song Y., Liu Q., Wang H., Zhu X. Effect of Gd on microstructure and stress corrosion cracking of the AZ91-extruded magnesium alloy. *Materials and Corrosion*, 2021, vol. 72, no. 7, pp. 1189–1200. DOI: [10.1002/maco.202112294](https://doi.org/10.1002/maco.202112294).
4. Peron M., Bertolini R., Ghiotti A., Torgersen J., Bruschi S., Berto F. Enhancement of stress corrosion cracking of AZ31 magnesium alloy in simulated body fluid thanks to cryogenic machining. *Journal of the Mechanical Behavior of Biomedical Materials*, 2020, vol. 101, article number 103429. DOI: [10.1016/j.jmbbm.2019.103429](https://doi.org/10.1016/j.jmbbm.2019.103429).
5. Merson E., Myagkikh P., Poluyanov V., Merson D., Vinogradov A. On the role of hydrogen in stress corrosion cracking of magnesium and its alloys: Gas-analysis study // *Materials Science and Engineering A*. 2019. Vol. 748. P. 337-346. DOI: [10.1016/j.msea.2019.01.107](https://doi.org/10.1016/j.msea.2019.01.107).
6. Chakrapani D.G., Pugh E.N. Hydrogen embrittlement in a Mg-Al alloy. *Metallurgical Transactions A*, 1976, vol. 7, no. 2, pp. 173–178. DOI: [10.1007/BF02644454](https://doi.org/10.1007/BF02644454).
7. Merson E., Poluyanov V., Myagkikh P., Merson D., Vinogradov A. On the role of pre-exposure time and corrosion products in stress-corrosion cracking of ZK60 and AZ31 magnesium alloys. *Materials Science and Engineering A*, 2021, vol. 806, article number 140876. DOI: [10.1016/j.msea.2021.140876](https://doi.org/10.1016/j.msea.2021.140876).
8. Stampella R.S., Procter R.P.M., Ashworth V. Environmentally-induced cracking of magnesium. *Corrosion Science*, 1984, vol. 24, no. 4, pp. 325–341. DOI: [10.1016/0010-938X\(84\)90017-9](https://doi.org/10.1016/0010-938X(84)90017-9).
9. Choudhary L., Singh Raman R.K. Magnesium alloys as body implants: Fracture mechanism under dynamic and static loadings in a physiological environment. *Acta Biomaterialia*, 2012, vol. 8, no. 2, pp. 916–923. DOI: [10.1016/j.actbio.2011.10.031](https://doi.org/10.1016/j.actbio.2011.10.031).
10. Bobby Kannan M., Dietzel W. Pitting-induced hydrogen embrittlement of magnesium-aluminium alloy. *Materials and Design*, 2012, vol. 42, pp. 321–326. DOI: [10.1016/j.matdes.2012.06.007](https://doi.org/10.1016/j.matdes.2012.06.007).
11. Jafari S., Raman R.K.S., Davies C.H.J. Stress corrosion cracking of an extruded magnesium alloy (ZK21) in a simulated body fluid. *Engineering Fracture Mechanics*, 2018, vol. 201, pp. 47–55. DOI: [10.1016/j.engfracmech.2018.09.002](https://doi.org/10.1016/j.engfracmech.2018.09.002).
12. Cai C., Song R., Wen E., Wang Y., Li J. Effect of microstructure evolution on tensile fracture behavior of

- Mg-2Zn-1Nd-0.6Zr alloy for biomedical applications. *Materials and Design*, 2019, vol. 182, article number 108038. DOI: [10.1016/j.matdes.2019.108038](https://doi.org/10.1016/j.matdes.2019.108038).
13. Jiang P., Blawert C., Bohlen J., Zheludkevich M.L. Corrosion performance, corrosion fatigue behavior and mechanical integrity of an extruded Mg4Zn0.2Sn alloy. *Journal of Materials Science and Technology*, 2020, vol. 59, pp. 107–116. DOI: [10.1016/j.jmst.2020.04.042](https://doi.org/10.1016/j.jmst.2020.04.042).
 14. Prabhu D.B., Nampoothiri J., Elakkiya V., Narmadha R., Selvakumar R., Sivasubramanian R., Gopalakrishnan P., Ravi K.R. Elucidating the role of microstructural modification on stress corrosion cracking of biodegradable Mg-4Zn alloy in simulated body fluid. *Materials Science and Engineering C*, 2020, vol. 106, article number 110164. DOI: [10.1016/j.msec.2019.110164](https://doi.org/10.1016/j.msec.2019.110164).
 15. Chen K., Lu Y., Tang H., Gao Y., Zhao F., Gu X., Fan Y. Effect of strain on degradation behaviors of WE43, Fe and Zn wires. *Acta Biomaterialia*, 2020, vol. 113, pp. 627–645. DOI: [10.1016/j.actbio.2020.06.028](https://doi.org/10.1016/j.actbio.2020.06.028).
 16. Merson E., Poluyanov V., Myagkikh P., Merson D., Vinogradov A. Effect of strain rate and corrosion products on pre-exposure stress corrosion cracking in the ZK60 magnesium alloy. *Materials Science and Engineering A*, 2022, vol. 830, article number 142304. DOI: [10.1016/j.msea.2021.142304](https://doi.org/10.1016/j.msea.2021.142304).
 17. Safyari M., Moshtaghi M., Kuramoto S. Effect of strain rate on environmental hydrogen embrittlement susceptibility of a severely cold-rolled Al-Cu alloy. *Vacuum*, 2020, vol. 172, article number 109057. DOI: [10.1016/j.vacuum.2019.109057](https://doi.org/10.1016/j.vacuum.2019.109057).
 18. Momotani Y., Shibata A., Terada D., Tsuji N. Effect of strain rate on hydrogen embrittlement in low-carbon martensitic steel. *International journal of hydrogen energy*, 2017, vol. 42, no. 5, pp. 3371–3379. DOI: [10.1016/j.ijhydene.2016.09.188](https://doi.org/10.1016/j.ijhydene.2016.09.188).
 19. Kappes M., Iannuzzi M., Carranza R.M. Pre-exposure embrittlement and stress corrosion cracking of magnesium alloy AZ31B in chloride solutions. *Corrosion*, 2014, vol. 70, no. 7, pp. 667–677. DOI: [10.5006/1172](https://doi.org/10.5006/1172).
 20. Merson E., Poluyanov V., Myagkikh P., Merson D., Vinogradov A. Effect of Air Storage on Stress Corrosion Cracking of ZK60 Alloy Induced by Preliminary Immersion in NaCl-Based Corrosion Solution. *Materials*, 2022, vol. 15, no. 21, article number 7862. DOI: [10.3390/ma15217862](https://doi.org/10.3390/ma15217862).
 21. Atrens A., Shi Z., Mehreen S.U., Johnston S., Song G.L., Chen X., Pan F. Review of Mg alloy corrosion rates. *Journal of magnesium and alloys*, 2020, vol. 8, no. 4, pp. 989–998. DOI: [10.1016/j.jma.2020.08.002](https://doi.org/10.1016/j.jma.2020.08.002).
 22. Lynch S.P., Trevena P. Stress corrosion cracking and liquid metal embrittlement in pure magnesium. *Corrosion*, 1988, vol. 44, no. 2, pp. 113–124. DOI: [10.5006/1.3583907](https://doi.org/10.5006/1.3583907).
 - Vol. 260. Article number 126920. DOI: [10.1016/j.matlet.2019.126920](https://doi.org/10.1016/j.matlet.2019.126920).
 2. Zhang X., Wu W., Fu H., Li J. The effect of corrosion evolution on the stress corrosion cracking behavior of mooring chain steel // *Corrosion Science*. 2022. Vol. 203. Article number 110316. DOI: [10.1016/j.corsci.2022.110316](https://doi.org/10.1016/j.corsci.2022.110316).
 3. Song Y., Liu Q., Wang H., Zhu X. Effect of Gd on microstructure and stress corrosion cracking of the AZ91-extruded magnesium alloy // *Materials and Corrosion*. 2021. Vol. 72. № 7. P. 1189–1200. DOI: [10.1002/maco.202112294](https://doi.org/10.1002/maco.202112294).
 4. Peron M., Bertolini R., Ghiotti A., Torgersen J., Bruschi S., Berto F. Enhancement of stress corrosion cracking of AZ31 magnesium alloy in simulated body fluid thanks to cryogenic machining // *Journal of the Mechanical Behavior of Biomedical Materials*. 2020. Vol. 101. Article number 103429. DOI: [10.1016/j.jmbbm.2019.103429](https://doi.org/10.1016/j.jmbbm.2019.103429).
 5. Merson E., Myagkikh P., Poluyanov V., Merson D., Vinogradov A. On the role of hydrogen in stress corrosion cracking of magnesium and its alloys: Gas-analysis study // *Materials Science and Engineering A*. 2019. Vol. 748. P. 337–346. DOI: [10.1016/j.msea.2019.01.107](https://doi.org/10.1016/j.msea.2019.01.107).
 6. Chakrapani D.G., Pugh E.N. Hydrogen embrittlement in a Mg-Al alloy // *Metallurgical Transactions A*. 1976. Vol. 7. № 2. P. 173–178. DOI: [10.1007/BF02644454](https://doi.org/10.1007/BF02644454).
 7. Merson E., Poluyanov V., Myagkikh P., Merson D., Vinogradov A. On the role of pre-exposure time and corrosion products in stress-corrosion cracking of ZK60 and AZ31 magnesium alloys // *Materials Science and Engineering A*. 2021. Vol. 806. Article number 140876. DOI: [10.1016/j.msea.2021.140876](https://doi.org/10.1016/j.msea.2021.140876).
 8. Stampella R.S., Procter R.P.M., Ashworth V. Environmentally-induced cracking of magnesium // *Corrosion Science*. 1984. Vol. 24. № 4. P. 325–341. DOI: [10.1016/0010-938X\(84\)90017-9](https://doi.org/10.1016/0010-938X(84)90017-9).
 9. Choudhary L., Singh Raman R.K. Magnesium alloys as body implants: Fracture mechanism under dynamic and static loadings in a physiological environment // *Acta Biomaterialia*. 2012. Vol. 8. № 2. P. 916–923. DOI: [10.1016/j.actbio.2011.10.031](https://doi.org/10.1016/j.actbio.2011.10.031).
 10. Bobby Kannan M., Dietzel W. Pitting-induced hydrogen embrittlement of magnesium-aluminium alloy // *Materials and Design*. 2012. Vol. 42. P. 321–326. DOI: [10.1016/j.matdes.2012.06.007](https://doi.org/10.1016/j.matdes.2012.06.007).
 11. Jafari S., Raman R.K.S., Davies C.H.J. Stress corrosion cracking of an extruded magnesium alloy (ZK21) in a simulated body fluid // *Engineering Fracture Mechanics*. 2018. Vol. 201. P. 47–55. DOI: [10.1016/j.engfracmech.2018.09.002](https://doi.org/10.1016/j.engfracmech.2018.09.002).
 12. Cai C., Song R., Wen E., Wang Y., Li J. Effect of microstructure evolution on tensile fracture behavior of Mg-2Zn-1Nd-0.6Zr alloy for biomedical applications // *Materials and Design*. 2019. Vol. 182. Article number 108038. DOI: [10.1016/j.matdes.2019.108038](https://doi.org/10.1016/j.matdes.2019.108038).
 13. Jiang P., Blawert C., Bohlen J., Zheludkevich M.L. Corrosion performance, corrosion fatigue behavior and mechanical integrity of an extruded Mg4Zn0.2Sn alloy //

СПИСОК ЛИТЕРАТУРЫ

1. Yu Z., Chen J., Yan H., Xia W., Su B., Gong X., Guo H. Degradation, stress corrosion cracking behavior and cytocompatibility of high strain rate rolled Mg-Zn-Sr alloys // *Materials Letters*. 2020.

- Journal of Materials Science and Technology. 2020. Vol. 59. P. 107–116. DOI: [10.1016/j.jmst.2020.04.042](https://doi.org/10.1016/j.jmst.2020.04.042).
14. Prabhu D.B., Nampoothiri J., Elakkiya V., Narmadha R., Selvakumar R., Sivasubramanian R., Gopalakrishnan P., Ravi K.R. Elucidating the role of microstructural modification on stress corrosion cracking of biodegradable Mg–4Zn alloy in simulated body fluid // Materials Science and Engineering C. 2020. Vol. 106. Article number 110164. DOI: [10.1016/j.msec.2019.110164](https://doi.org/10.1016/j.msec.2019.110164).
 15. Chen K., Lu Y., Tang H., Gao Y., Zhao F., Gu X., Fan Y. Effect of strain on degradation behaviors of WE43, Fe and Zn wires // Acta Biomaterialia. 2020. Vol. 113. P. 627–645. DOI: [10.1016/j.actbio.2020.06.028](https://doi.org/10.1016/j.actbio.2020.06.028).
 16. Merson E., Poluyanov V., Myagkikh P., Merson D., Vinogradov A. Effect of strain rate and corrosion products on pre-exposure stress corrosion cracking in the ZK60 magnesium alloy // Materials Science and Engineering A. 2022. Vol. 830. Article number 142304. DOI: [10.1016/j.msea.2021.142304](https://doi.org/10.1016/j.msea.2021.142304).
 17. Safyari M., Moshtaghi M., Kuramoto S. Effect of strain rate on environmental hydrogen embrittlement susceptibility of a severely cold-rolled Al–Cu alloy // Vacuum. 2020. Vol. 172. Article number 109057. DOI: [10.1016/j.vacuum.2019.109057](https://doi.org/10.1016/j.vacuum.2019.109057).
 18. Momotani Y., Shibata A., Terada D., Tsuji N. Effect of strain rate on hydrogen embrittlement in low-carbon martensitic steel // International journal of hydrogen energy. 2017. Vol. 42. № 5. P. 3371–3379. DOI: [10.1016/j.ijhydene.2016.09.188](https://doi.org/10.1016/j.ijhydene.2016.09.188).
 19. Kappes M., Iannuzzi M., Carranza R.M. Pre-exposure embrittlement and stress corrosion cracking of magnesium alloy AZ31B in chloride solutions // Corrosion. 2014. Vol. 70. № 7. P. 667–677. DOI: [10.5006/1172](https://doi.org/10.5006/1172).
 20. Merson E., Poluyanov V., Myagkikh P., Merson D., Vinogradov A. Effect of Air Storage on Stress Corrosion Cracking of ZK60 Alloy Induced by Preliminary Immersion in NaCl-Based Corrosion Solution // Materials. 2022. Vol. 15. № 21. Article number 7862. DOI: [10.3390/ma15217862](https://doi.org/10.3390/ma15217862).
 21. Atrens A., Shi Z., Mehreen S.U., Johnston S., Song G.L., Chen X., Pan F. Review of Mg alloy corrosion rates // Journal of magnesium and alloys. 2020. Vol. 8. № 4. P. 989–998. DOI: [10.1016/j.jma.2020.08.002](https://doi.org/10.1016/j.jma.2020.08.002).
 22. Lynch S.P., Trevena P. Stress corrosion cracking and liquid metal embrittlement in pure magnesium // Corrosion. 1988. Vol. 44. № 2. P. 113–124. DOI: [10.5006/1.3583907](https://doi.org/10.5006/1.3583907).

Влияние скорости деформирования на механические свойства и характер разрушения сплава AZ31 и технически чистого магния, предварительно выдержанных в коррозионной среде

© 2023

Мерсон Евгений Дмитриевич^{*1}, кандидат физико-математических наук, старший научный сотрудник НИИ прогрессивных технологий

*Полюянов Виталий Александрович*², кандидат технических наук, младший научный сотрудник НИИ прогрессивных технологий

*Мягких Павел Николаевич*³, младший научный сотрудник НИИ прогрессивных технологий

*Мерсон Дмитрий Львович*⁴, доктор физико-математических наук, профессор, директор НИИ прогрессивных технологий

Тольяттинский государственный университет, Тольятти (Россия)

*E-mail: Mersoned@gmail.com¹ORCID: <https://orcid.org/0000-0002-7063-088X>²ORCID: <https://orcid.org/0000-0002-0570-2584>³ORCID: <https://orcid.org/0000-0002-7530-9518>⁴ORCID: <https://orcid.org/0000-0001-5006-4115>

Поступила в редакцию 15.11.2022

Принята к публикации 02.12.2022

Аннотация: Магниево-цинковые сплавы являются перспективными материалами для использования в авиации, автомобилестроении и медицине, однако, вследствие низкой стойкости к коррозионному растрескиванию под напряжением (КРН), область их применения ограничена. Для создания сплавов, обладающих высокой стойкостью к КРН, требуется всестороннее изучение природы этого явления. Ранее было высказано предположение, что важную роль в механизме КРН может играть диффузионно-подвижный водород и продукты коррозии, образующиеся на поверхности магния. Однако вклад каждого из этих факторов в охрупчивание магния и его сплавов, вызванное КРН, мало изучен. Поскольку влияние диффузионно-подвижного водорода на механические свойства металлов усиливается с уменьшением скорости деформирования, актуальной задачей является исследование скоростной чувствительности восприимчивости сплавов магния к КРН. В настоящей работе исследовались технически чистый магний в литом состоянии и сплав AZ31: изучалось влияние скорости деформирования в диапазоне от $5 \cdot 10^{-6}$ до $5 \cdot 10^{-4} \text{ с}^{-1}$ на механические свойства, состояние боковой поверхности и излома материалов до и после выдержки в коррозионной среде и после удаления продуктов коррозии. Установлено, что предварительная выдержка в коррозионной среде приводит к охрупчиванию сплава AZ31, но не влияет на механические свойства и характер

разрушения чистого магния. Обнаружено, что охрупчивание сплава AZ31, вызванное предварительной выдержкой в коррозионной среде, проявляется в полной мере только при низкой скорости деформирования и только в том случае, если на поверхности образцов присутствует слой продуктов коррозии. Показано, что изменение скорости деформирования оказывает незначительное влияние на свойства чистого магния. Сделан вывод о том, что основной причиной охрупчивания сплава AZ31 после выдержки в коррозионной среде является слой продуктов коррозии, который, предположительно, содержит охрупчивающие агенты, такие как водород и остаточная коррозионная среда.

Ключевые слова: магниевые сплавы; AZ31; магний; коррозионное растрескивание под напряжением; коррозия; скорость деформирования; механические свойства.

Благодарности: Исследование выполнено при финансовой поддержке РФФИ в рамках научного проекта № 18-19-00592.

Для цитирования: Мерсон Е.Д., Полуянов В.А., Мягких П.Н., Мерсон Д.Л. Влияние скорости деформирования на механические свойства и характер разрушения сплава AZ31 и технически чистого магния, предварительно выдержанных в коррозионной среде // Frontier Materials & Technologies. 2023. № 3. С. 71–82. DOI: 10.18323/2782-4039-2023-3-65-7.